Evolution of Enzymatic Activities in the Orotidine 5′-Monophosphate Decarboxylase Suprafamily: Enhancing the Promiscuous D-*arabino*-Hex-3-ulose 6-Phosphate Synthase Reaction Catalyzed by 3-Keto-L-gulonate 6-Phosphate Decarboxylase†

Wen Shan Yew,‡ Julie Akana,‡ Eric L. Wise,§ Ivan Rayment,*,§ and John A. Gerlt*,‡

Departments of Biochemistry and Chemistry, University of Illinois, Urbana, Illinois 61801, and Department of Biochemistry, University of Wisconsin, Madison, Wisconsin 53706

Received October 12, 2004; Revised Manuscript Received November 16, 2004

ABSTRACT: 3-Keto-L-gulonate 6-phosphate decarboxylase (KGPDC) and D-*arabino*-hex-3-ulose 6-phosphate synthase (HPS) are members of the orotidine 5′-monophosphate decarboxylase (OMPDC) suprafamily [Wise, E., Yew, W. S., Babbitt, P. C., Gerlt, J. A., and Rayment, I. (2002) *Biochemistry 41*, 3861−3869], a group of homologous enzymes that share the $(\beta/\alpha)_8$-barrel fold. KGPDC catalyzes a Mg^{2+}-dependent decarboxylation reaction in the catabolic pathway of L-ascorbate utilization by *Escherichia coli* K-12 [Yew, W. S., and Gerlt, J. A. (2002) *J.Bacteriol. 184*, 302−306]; HPS catalyzes a Mg^{2+}-dependent aldol condensation between formaldehyde and D-ribulose 5-phosphate in formaldehyde-fixing methylotrophic bacteria [Kato, N., Ohashi, H., Hori, T., Tani, Y., and Ogata, K. (1977) *Agric. Biol. Chem. 41*, 1133−1140]. Our previous studies of the KGPDC from *E. coli* established the occurrence of a stabilized *cis*-enediolate intermediate [Yew, W. S., Wise, E., Rayment, I., and Gerlt, J. A. (2004) *Biochemistry 43*, 6427−6437; Wise, E., Yew, W. S., Gerlt, J. A., and Rayment, I. (2004) *Biochemistry 43*, 6438−6446]. Although the mechanism of the HPS-catalyzed reaction has not yet been investigated, it also is expected to involve a Mg^{2+}-stabilized *cis*-enediolate intermediate. We now have discovered that the KGPDC from *E. coli* and the HPS from *Methylomonas aminofaciens* are both naturally promiscuous for the reaction catalyzed by the homologue. On the basis of the alignment of the sequences of orthologous KGPDC's and HPS's, four conserved active site residues in the KGPDC from *E. coli* were mutated to those conserved in HPS's (E112D/R139V/T169A/R192A): the value of the k_{cat} for the promiscuous HPS activity was increased as much as 170-fold (for the E112D/R139V/T169A/R192A mutant), and the value of k_{cat}/K_m was increased as much as 260-fold (for the E112D/R139V/T169A mutant); in both cases, the values of the kinetic constants for the natural KGPDC activity were decreased. Together with the structures of mutants reported in the accompanying manuscript [Wise, E. L., Yew, W. S., Akana, J., Gerlt, J. A., and Rayment, I., accompanying manuscript], these studies illustrate that large changes in catalytic efficiency can be accomplished with only modest changes in active site structure. Thus, the $(\beta/\alpha)_8$-barrel fold shared by members of the OMPDC suprafamily appears well-suited for the evolution of new functions.

The $(\beta/\alpha)_8$-barrel is one of the most abundant folds in enzymes, comprising at least 10% of the protein structures in the Protein Data Bank (*1*). In this fold, the active sites are always located at the C-terminal ends of the β-strands, where they can be mutated to accomplish evolution of new functions. Various strategies have been proposed for such evolutionary processes, including "gene sharing" in which a gene encodes a functionally promiscuous protein, so that after gene duplication selective pressure coupled with a small number of mutations can enhance the level of the unnatural activity to generate a new enzymatic function (*2*). Several examples have been described that illustrate the likely importance of naturally occurring promiscuity in the evolution of function in mechanistically diverse superfamilies whose members share a common partial reaction (*3*).

The members of the orotidine 5′-monophosphate decarboxylase (OMPDC)[1] suprafamily share the $(\beta/\alpha)_8$-barrel fold (*4*). Two mechanistically diverse members of the suprafamily, 3-keto-L-gulonate 6-phosphate decarboxylase (KGPDC) and D-*arabino*-hex-3-ulose 6-phosphate synthase (HPS), catalyze different overall reactions that are expected to share Mg^{2+}-assisted stabilization of 1,2-enediolate intermediates (Figure 1). KGPDC catalyzes the decarboxylation of 3-keto-

† This research was supported by Grant GM-65155 (to J.A.G. and I.R.) from the National Institutes of Health..

* To whom correspondence should be addressed. J.A.G.: Department of Biochemistry, University of Illinois, 600 South Mathews Avenue, Urbana, IL 61801; phone, (217) 244-7414; fax, (217) 265-0385; e-mail, j-gerlt@uiuc.edu. I.R.: Department of Biochemistry, University of Wisconsin, 433 Babcock Drive, Madison, WI 53706; phone, (608) 262-0437; fax, (608) 262-1319; e-mail, Ivan_Rayment@biochem.wisc.edu.

‡ University of Illinois.

§ University of Wisconsin.

[1] Abbreviations: βKGP, 3-keto-L-gulonate 6-phosphate; DR5P, D-ribulose 5-phosphate; HPS, D-*arabino*-hex-3-ulose 6-phosphate synthase; KGPDC, 3-keto-L-gulonate 6-phosphate decarboxylase; LX5P, L-xylulose 5-phosphate; LyxK, 2,3-diketo-L-gulonate kinase; OMPDC, orotidine 5′-monophosphate decarboxylase; XylA, D-xylose isomerase; XylB, D-xylulokinase; YiaK, 2,3-diketo-L-gulonate reductase.

10.1021/bi047815v CCC: $30.25
Published on Web 01/22/2005

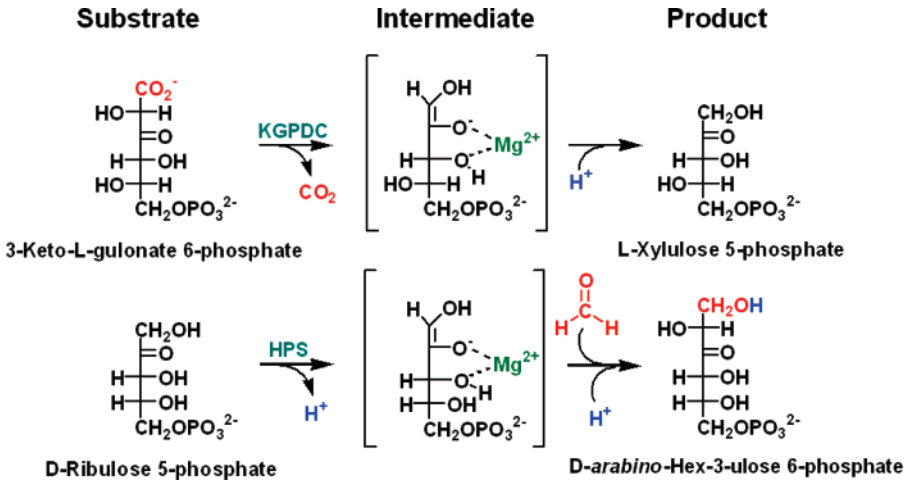

FIGURE 1: Reactions catalyzed by KGPDC and HPS.

L-gulonate 6-phosphate, an intermediate in the utilization of L-ascorbate by *Escherichia coli* K-12 (*5*) and other bacteria; HPS catalyzes the aldol condensation of D-ribulose 5-phosphate with formaldehyde in methylotrophic bacteria (*6*). The sequences of the HPS's and KGPDC's are approximately 30% identical. In this manuscript, we report naturally occurring promiscuity catalyzed by both the KGPDC from *E. coli* and the HPS from *Methylomonas aminofaciens*: HPS catalyzes the KGPDC reaction with strikingly high efficiency, and KGPDC catalyzes the HPS reaction with low efficiency.

Our previous mechanistic and structural studies have yielded much information about structure/function relationships for the reaction catalyzed by the KGPDC from *E. coli*. KGPDC is a dimer of $(\beta/\alpha)_8$-barrels, with the active site located at the interface of the component polypeptides (*4*). Conserved carboxylate groups at the C-terminal ends of the first, second, and third β-strands bind the essential Mg^{2+} that stabilizes the *cis*-1,2-enediolate intermediate generated by decarboxylation (*7*). Surprisingly, our studies of the KGPDC from *E. coli* provided evidence that the intermediate is competitively protonated by two water molecules located on opposite faces of the intermediate to yield the prochiral hydroxymethylene group of the L-xylulose 5-phosphate product (*8*, *9*). His 136 and Arg 139, located in a loop at the C-terminal end of the sixth β-strand and conserved in all KGPDC's, modulate the positions and acidities of the proximal water molecules that protonate the intermediate.

To date, we have been unable to obtain crystals of a HPS that are suitable for structural determination; as a result, our knowledge of structure/function relationships for the HPS-catalyzed reaction is not as advanced as that for the KGPDC-catalyzed reaction. The HPS reaction also requires Mg^{2+} (*6*), so we assume that the metal ion is coordinated by conserved homologues of the metal-ion binding ligands located at the ends of the second and third β-strands in the active site of KGPDC. Furthermore, the sequences of all HPS's that can be identified in the databases contain a homologue of the catalytic His in the loop at the end of the sixth β-strand in KGPDC. The homologue of this residue, His 136, is essential for catalyzing the stereospecific exchange of one proton of the hydroxymethylene group of the L-xylulose 5-phosphate product with solvent hydrogen (*8*). Therefore, we hypothesize that the conserved His in HPS's is essential for initiating the aldol condensation by stereospecifically abstracting a proton from the 1-hydroxymethylene group of D-ribulose 5-phosphate to initiate the formation of D-*arabino*-hex-3-ulose 6-phosphate.

In addition, comparisons of sequence alignments of the available sequences for KGPDC's and HPS's reveal the presence of several conserved residues in each orthologue that can be associated with the different reactions (Figure 2). These differences, together with the expected similar structures of the enediolate intermediates in both reactions, suggested that we might be able to enhance the inefficient promiscuous HPS activity catalyzed by the KGPDC from *E. coli* by changing the identities of the conserved active site residues in KGPDC's to those conserved in HPS's. Substantial enhancement of the promiscuous HPS activity is achieved with no more than four substitutions and is accompanied by a modest decrease in KGPDC activity, thereby providing insights into possible pathways for divergent evolution of function in the OMPDC suprafamily.

MATERIALS AND METHODS

^1H NMR spectra were recorded using a Varian Unity INOVA 500NB MHz NMR spectrometer; ^{13}C and ^{31}P NMR spectra were recorded using a Varian Unity 500 MHz NMR spectrometer. All reagents were the highest quality grade commercially available.

Cloning and Expression of HPS. The gene encoding HPS from *M. aminofaciens* was subcloned from pUH1 (*10*) using Platinum *Pfx* DNA polymerase (Life Technologies). pUH1, a kind gift from Professor Nobuo Kato, is a modified pUC118 plasmid containing the gene encoding HPS from *M. aminofaciens*. The PCR reaction (100 μL) contained 1 ng of plasmid DNA, 10 μL of 10X *Pfx* amplification buffer (Life Technologies), 1 mM $MgSO_4$, 0.4 mM of each dNTP, 40 pmol of each primer (forward primer 5′-GGAATTC-CATATGGCATTGACACAAATGGC-3′ and reverse primer 5′-CCGGCCTCGAGTTACTTAGCCAGGCC-3′), and 5 units of Platinum *Pfx* DNA polymerase. The gene was amplified using a PTC-200 gradient thermal cycler (MJ Research), with the following parameters: 94 °C for 2 min followed by 40 cycles of 94 °C for 1 min, a gradient temperature range of 45−60 °C for 1 min and 15 s, 68 °C for 2 min, and a final extension of 68 °C for 10 min. The amplified gene was

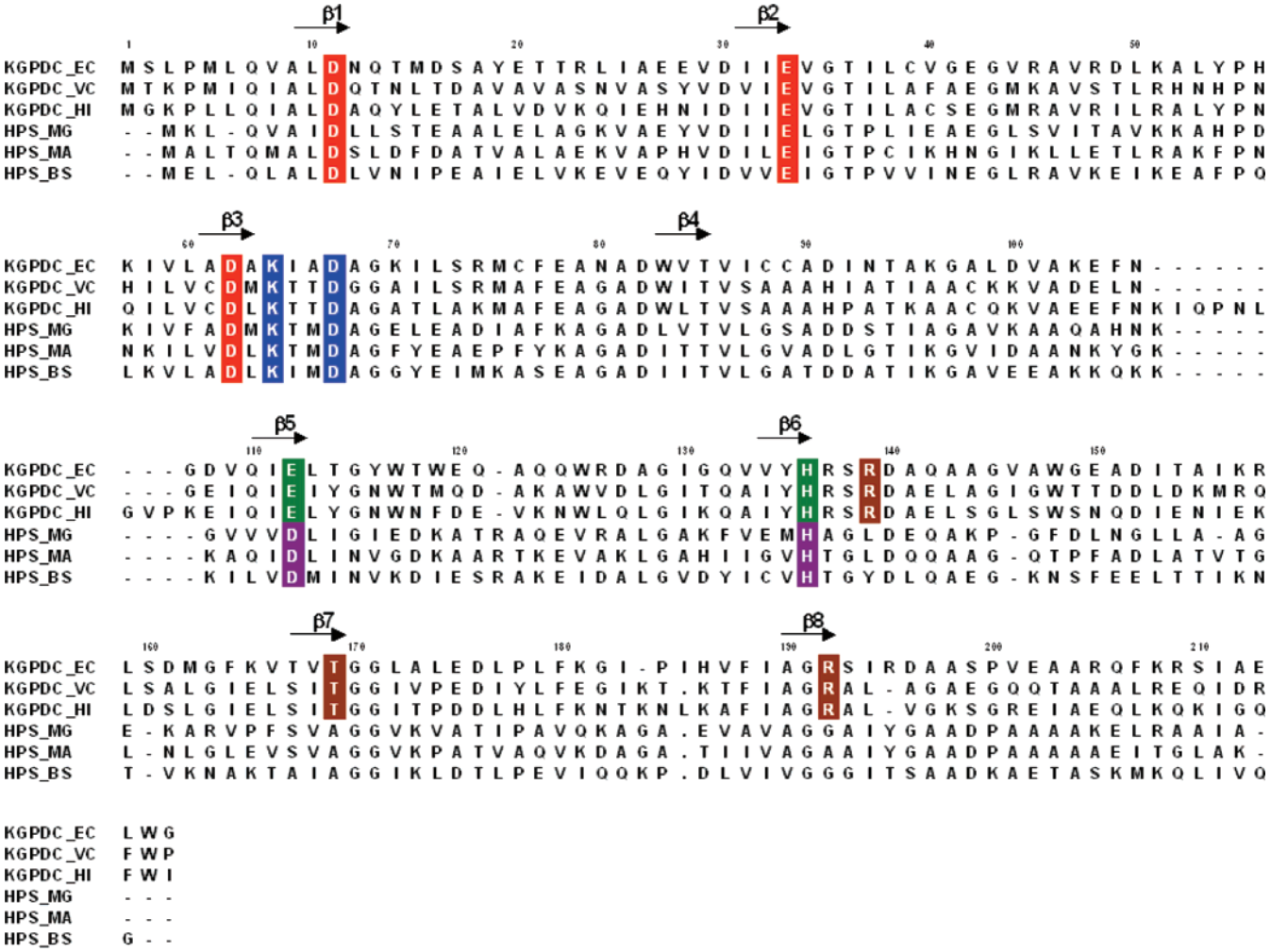

FIGURE 2: Sequence alignment of KGPDC's from *E. coli* (KGPDC_EC), *Vibrio cholera* (KGPDC_VC), and *Haemophilus influenza* (KGPDC_HI); and HPS's from *Mycobacterium gastri* (HPS_MG), *M. aminofaciens* (HPS_MA), and *B. subtilis* (HPS_BS). The strictly conserved Mg^{2+} ligands, Asp 11, Glu 33 and Asp 62, are highlighted in red. Lys 64 and Asp 67, residues involved in binding and stabilizing the *cis*-enediolate intermediate, are highlighted in blue. The His 136-Glu 112 dyads in the KGPDC's are highlighted in green, and the presumed His-Asp dyads in the HPS's are highlighted in magenta. In addition to Glu 112, the residues strictly conserved in KGPDC's that were targeted for mutagenesis, Arg 139, Thr 169, and Arg 192, are highlighted in brown. The alignment was produced by the Pileup algorithm of the GCG software package. Residues are numbered according to the KGPDC_EC sequence. The sequence identity between KGPDC's and HPS's is approximately 30%.

subcloned into a modified pKK223-3 (Amersham) vector in which the N-terminus contained ten His residues and the recombinant protein was expressed in a KGPDC-deficient *E. coli* strain (*8*). Transformed cells were grown at 25 °C in LB broth (supplemented with 100 μg/mL ampicillin) for 48 h and harvested by centrifugation. No IPTG was added to induce protein expression. HPS from *M. aminofaciens* was purified as previously described for wild-type KGPDC (*7*).

Site-Directed Mutagenesis and Protein Purification. UlaD, the gene encoding KGPDC in *E. coli*, was previously subcloned into a modified pKK223-3 (Amersham) vector in which the N-terminus contained ten His residues. Site-directed mutants of KGPDC were constructed as previously described using the QuikChange kit (Stratagene) (*8*). Mutants of KGPDC were verified by sequencing and expressed in a KGPDC-deficient strain of *E. coli* and purified as previously described for wild-type KGPDC.

Synthesis of D*-Ribulose 5-Phosphate.* The gene encoding D-ribulokinase was cloned from genomic DNA isolated from *E. coli* strain MG1655 and expressed using a modified pET15-b vector encoding an N-terminal His tag with ten His residues in *E. coli* strain BL21(DE3) and purified as described for KGPDC.

D-Ribulose was prepared according to the method of Touster et al. (*11*), with the following modifications: 15 g of D-ribose was refluxed under dry conditions in 150 mL of distilled pyridine for 5 h. Pyridine was removed by evaporation, and unreacted D-ribose was removed using a separation funnel after extraction with ethanol and ether. D-Ribulose 5-phosphate was prepared from D-ribulose using D-ribulokinase. The reaction mixture (250 mL) contained 40 mM D-ribulose (10 mmol), 0.76 mM ATP, 13 mM $MgCl_2$, 50 mM K^+HEPES, pH 7.5, 31.7 mM acetyl phosphate (7.9 mmol), 300 units of D-ribulokinase, and 400 units of acetate kinase. After incubation for 3 h at 25 °C, nucleotides were removed by treatment with activated charcoal, and the enzymes were removed by filtration through a Biomax-10 (10000 Da) ultrafiltration membrane (Millipore). D-Ribulose 5-phosphate was purified by passing the resulting solution through a column of DEAE Sepharose Fast Flow (HCO_3^- form) and eluting with triethylammonium bicarbonate (pH 8.0). Fractions containing D-ribulose 5-phosphate were

pooled, and triethylammonium bicarbonate was removed by evaporation. ^{1}H NMR (D_2O, 500 MHz): δ 4.44 (q, $J = 19.4$ Hz, 2H), δ 4.26 (d, $J = 6.0$ Hz, 1H), δ 3.84 (q, $J = 4.9$ Hz, 1H), δ 3.72 (m, 2H). ^{13}C NMR (D_2O, 500 MHz): δ 212.6, 74.7, 71.9, 66.5, 63.6.

Assay of HPS. Proteins were assayed for HPS activity at 25 °C as previously described (*12*), with the following modifications: the reaction mixture (200 μL) contained D-ribulose 5-phosphate (0.0625 to 160 mM), 50 mM potassium phosphate buffer, pH 7.0, 5 mM $MgCl_2$, 0.4 mM $NADP^+$, 5 mM formaldehyde, 20 μg of recombinant phosphohexulose isomerase (PHI) purified from *E. coli* BL21-(DE3) overproducing the PHI (YckF) from *Bacillus subtilis* (*13*), 1 unit of glucose 6-phosphate dehydrogenase, 1 unit of phosphoglucose isomerase, and HPS. The change in absorbance at 340 nm was measured.

Assay of KGPDC. Proteins were assayed for KGPDC activity as previously described (*5*). Briefly, a stock solution of 3-keto-L-gulonate 6-phosphate was generated in situ by incubating 2,3-diketo-L-gulonate (3.0 to 6.0 mM), 10 mM $MgCl_2$, ATP (6 to 10 mM), 80 units/mL of YiaK, 80 units/mL of LyxK, and an equivalent of NADH for 10 min at 25 °C. The assay mixtures (1 mL) contained 3-keto-L-gulonate 6-phosphate (0.078 to 5.0 mM), 50 mM K^+HEPES (pH 7.5), and 10 mM $MgCl_2$. After incubation at 25 °C for sufficient time to convert $\leq$10% of the substrate to product, the enzymes were removed by centrifugation through a Biomax-10 (10000 Da) Millipore centrifugal device. The L-xylulose 5-phosphate product was dephosphorylated by incubation with calf intestinal alkaline phosphatase (CIAP) at 37 °C for 5 min. CIAP was precipitated from the mixture by addition of 300 μL each of a 5% solution of $ZnSO_4 \cdot 7H_2O$ and of 0.15 M $Ba(OH)_2$. The supernatant was assayed for L-xylulose by reaction with L-cysteine and carbazole and measuring the absorbance at 540 nm (*14*).

Identification of the D-arabino-Hex-3-ulose 6-Phosphate Product Formed by the Aldol Condensation of D-Ribulose 5-Phosphate and Formaldehyde. The formation of D-*arabino*-hex-3-ulose 6-phosphate from D-ribulose 5-phosphate and formaldehyde catalyzed by either HPS or the E112D/R139V/T169A mutant of KGPDC was performed in a D_2O-containing buffer at 20 °C, with ^{1}H NMR spectra recorded as a function of time. A typical reaction contained 20 mM D-ribulose 5-phosphate, 50 mM K^+HEPES, pD 7.5, 10 mM $MgCl_2$, 18.75 mM formaldehyde (generated from a 1 M stock of paraformaldehyde in D_2O), and enzyme. All enzymes were exchanged into D_2O buffer (50 mM K^+HEPES, pD 7.5) using an Amicon (10000 Da) stirred ultrafiltration cell.

Exchange of the 1-Hydroxymethylene Group of D-Ribulose 5-Phosphate and L-Xylulose 5-Phosphate. D-Ribulose 5-phosphate was incubated with wild-type KGPDC, mutant KGPDC, or HPS in D_2O buffer at 20 °C, and ^{1}H NMR spectra were recorded as a function of time. A typical reaction contained 20 mM D-ribulose 5-phosphate, 50 mM K^+HEPES, pD 7.5, 10 mM $MgCl_2$, and enzyme. The rate of proton exchange, k_{exc}, of the 1-hydroxymethylene group by enzyme was calculated from eq 1, which takes into account the total amount of D-ribulose 5-phosphate bound at any time,

$$k_{exc} = k_{obs}[DR5P]_T/[DR5P]_B \quad (1)$$

where k_{obs} is the observed first-order rate constant, $[DR5P]_T$ is the total D-ribulose 5-phosphate concentration, and $[DR5P]_B$ is the concentration of bound D-ribulose 5-phosphate. Since the concentration of D-ribulose 5-phosphate (20 mM) was significantly higher than the enzyme concentration (5 μM), the concentration of bound D-ribulose 5-phosphate ($[DR5P]_B$) was equal to the enzyme concentration used. L-Xylulose 5-phosphate was synthesized as previously described (*14*) and was used in the determination of the rate of proton exchange, k_{exc}, of the 1-hydroxymethylene group as previously described.

Formaldehyde as an Alternate Electrophile during Exchange of the 1-Hydroxymethylene Group of L-Xylulose 5-Phosphate. L-Xylulose 5-phosphate was incubated with HPS, wild-type KGPDC, or E112D/R139V/T169A mutant in D_2O buffer at 20 °C in the presence of formaldehyde, and ^{1}H NMR spectra were recorded as a function of time. A typical reaction contained 20 mM L-xylulose 5-phosphate, 50 mM K^+HEPES, pD 7.5, 10 mM $MgCl_2$, 18.75 mM formaldehyde, and enzyme.

Stereochemical Course of 3-Keto-L-gulonate 6-Phosphate Decarboxylation. 3-Keto-L-gulonate 6-phosphate was generated as previously described, and decarboxylated in a D_2O-containing buffer at 20 °C, with ^{1}H NMR spectra recorded as a function of time after initiation of the reaction. A typical reaction contained 20 mM 2,3-diketo-L-gulonate, 50 mM K^+HEPES, pD 7.5, 10 mM $MgCl_2$, 0.25 mM ATP, 0.25 mM NADH, 20 mM sodium formate, 20 mM acetyl phosphate, 150 units of 2,3-diketo-L-gulonate reductase (YiaK), 50 units of LyxK, 10 units of formate dehydrogenase, 20 units of acetate kinase, and 5 μM wild-type KGPDC (or increased amounts of mutant enzymes or HPS).

Formaldehyde as an Alternate Electrophile in Decarboxylation. 3-Keto-L-gulonate 6-phosphate was generated in situ as previously described and decarboxylated in a D_2O-containing buffer at 20 °C in the presence of formaldehyde, with ^{1}H NMR spectra recorded as a function of time after initiation of the reaction. A typical reaction contained all previously described components with the addition of 3.75 mM to 37.5 mM formaldehyde (generated from a 1 M stock of paraformaldehyde in D_2O).

RESULTS AND DISCUSSION

Natural Promiscuity of KGPDC for the HPS Reaction. We previously demonstrated that KGPDC catalyzes the stereospecific exchange of the pro*S* proton of the 1-hydroxymethylene group of its L-xylulose 5-phosphate product with solvent ($k_{exc} = 0.96$ s^{-1}, Table 1) (*8*). KGPDC also catalyzes the less efficient, but stereospecific, exchange of one proton of the 1-hydroxymethylene group of D-ribulose 5-phosphate ($k_{exc} = 1.3 \times 10^{-3}$ s^{-1}, Table 1).

We also previously demonstrated that KGPDC can catalyze an aldol condensation with formaldehyde using the enediolate intermediates obtained either by incubation with L-xylulose 5-phosphate or by decarboxylation of 3-keto-L-gulonate 6-phosphate, with the latter condensation effectively competing with protonation to generate the L-xylulose 5-phosphate product (*8*). Therefore, the ability of KGPDC to catalyze an exchange reaction with D-ribulose 5-phosphate led us to hypothesize that KGPDC could catalyze the "natural" HPS reaction using D-ribulose 5-phosphate. This expectation was realized, and the kinetic constants for the

Table 1: Rates of Exchange, Aldol, and Decarboxylation Reactions

			aldol			decarboxylation		
		exchange k_{exc} (s^{-1})	k_{cat} (s^{-1})	K_M (mM)	k_{cat}/K_M (M^{-1} s^{-1})	k_{cat} (s^{-1})	K_M (mM)	k_{cat}/K_M (M^{-1} s^{-1})
KGPDC	DR5P [a]	0.0013	0.0021	25	8.2×10^{-2}			
	LX5P [b]	0.96	0.32[d]					
	βKGP [c]					51	0.67	7.7×10^4
HPS	DR5P	4.4	7.4	0.46	1.6×10^4			
	LX5P	2.8	1.2[d]					
	βKGP					~15	5.4	2.3×10^3
E112D/R139V/T169A	DR5P	0.06	0.11	5.2	21			
	LX5P	0.2	0.11[d]					
	βKGP					2.4	0.91	2.6×10^3
E112D/R139V/T169A/R192A	DR5P	0.027	0.36	40	9			
	LX5P	0.18	0.014[d]					
	βKGP					*e*	*e*	1.5×10^2

[a] DR5P, D-ribulose 5-phosphate. [b] LX5P, L-xylulose 5-phosphate. [c] βKGP, 3-keto-L-gulonate 6-phosphate. [d] Apparent k_{cat}, measured at a high substrate concentration. [e] Saturation kinetics could not be attained.

natural and promiscuous aldol-condensation reactions catalyzed by KGPDC are displayed in Table 1. That KGPDC can catalyze a low level of the HPS reaction contrasts with a previous report that this enzyme cannot catalyze the HPS reaction (*13*).

Natural Promiscuity of HPS for the KGPDC Reaction. We expected that HPS would be able to generate and stabilize a 1,2-enediolate intermediate derived from its natural substrate, D-ribulose 5-phosphate, because this intermediate is expected to be the nucleophile for the aldol-condensation reaction with formaldehyde. This was confirmed by the ability of HPS to catalyze the facile exchange of one proton of the 1-hydroxymethylene group of D-ribulose 5-phosphate with solvent (Table 1). We also determined that HPS can generate a 1,2-enediolate intermediate derived from L-xylulose 5-phosphate, as judged by the facile exchange of its 1-pro*S* proton with solvent. Remarkably, HPS catalyzes exchange of one proton of the 1-hydroxymethylene group of the natural D-ribulose 5-phosphate and the promiscuous L-xylulose 5-phosphate at comparable rates (Table 1), in contrast to the markedly different exchange rates catalyzed by KGPDC.

Catalysis of the decarboxylation of 3-keto-L-gulonate 6-phosphate by KGPDC requires "only" that the active site bind the substrate and stabilize the 1,2-enediolate intermediate. Given that HPS can generate and stabilize the 1,2-enediolate intermediate derived from L-xylulose 5-phosphate, we were not surprised that it also catalyzes an efficient KGPDC reaction (Table 1).

Thus, both KGPDC from *E. coli* and HPS from *M. aminofaciens* are functionally promiscuous, each catalyzing two different overall reactions that involve formation and stabilization of diastereomeric 1,2-enediolate intermediates.

We cannot evaluate whether either HPS or KGPDC can catalyze the decarboxylation of 3-keto-D-altronate 6-phosphate, the 5-epimer of 3-keto-L-gulonate 6-phosphate, that would involve formation and stabilization of the 1,2-enediolate of D-ribulose 5-phosphate. 3-Keto-L-gulonate 6-phosphate is obtained by a series of enzymatic transformations starting with 2,3-diketo-L-gulonate, and these enzymes cannot be used to obtain the diastereomeric D-hex-3-ulose 6-phosphate.

Reactivities of the Enediolate Intermediates Generated by HPS and KGPDC. The values of the apparent k_{cat}'s for the aldol condensations catalyzed by KGPDC and HPS using L-xylulose 5-phosphate, 0.32 s^{-1} and 1.2 s^{-1}, respectively (Table 1), are comparable to the rates of exchange, k_{exc}, of the 1-pro*S* proton of the 1-hydroxymethylene group of L-xylulose 5-phosphate, 0.96 s^{-1} and 2.8 s^{-1}, respectively (Table 1). Similarly, the values of the apparent k_{cat}'s for the aldol condensations catalyzed by KGPDC and HPS using D-ribulose 5-phosphate, 2.1×10^{-3} s^{-1} and 7.4 s^{-1}, respectively (Table 1), are comparable to the rates of exchange, k_{exc}, of the 1-pro*S* proton of the 1-hydroxymethylene group of D-ribulose 5-phosphate, 1.3×10^{-3} s^{-1} and 4.4 s^{-1}, respectively (Table 1).

Thus, in both active sites, reaction of the 1,2-enediolate intermediate with formaldehyde effectively competes with protonation so that the rates of the aldol reactions likely reflect the rates of formation of the intermediates by proton abstraction.

Products of the Aldol Condensations Catalyzed by HPS and KGPDC. The aldol condensations of D-ribulose 5-phosphate and formaldehyde catalyzed by both KGPDC and HPS produce the same diastereomer of the D-hex-3-ulose 6-phosphate product, previously assigned as the *arabino* diastereomer for the HPS-catalyzed reaction (Figure 3) (*15*). Also, the aldol condensations of L-xylulose 5-phosphate with formaldehyde catalyzed by both enzymes yield the same diastereomer of the L-hex-3-ulose 6-phosphate product, presumably also the *arabino* diasterereomer (Figure 4), although we have not unambiguously determined its configuration. Thus, the same face (*re*) of C1 of the diastereomeric 1,2-enediolate intermediate derived from D-ribulose 5-phosphate or L-xylulose 5-phosphate apparently is available for reaction with formaldehyde in each active site.

Design of the KGPDC Scaffold for Enhanced HPS Activity. The promiscuous ability of KGPDC to catalyze low levels of the HPS reaction and the nearly equivalent rates of reaction of the stabilized enediolate intermediates derived from L-xylulose 5-phosphate and D-ribulose 5-phosphate with formaldehyde suggested that we might be able to enhance the promiscuity for the HPS reaction by increasing the rate of formation of the enediolate intermediate from D-ribulose 5-phosphate. We sought to accomplish this by "rational design". In the present absence of a high-resolution structure for any HPS, we used information derived from sequence alignments to enhance the HPS activity catalyzed by the KGPDC scaffold.

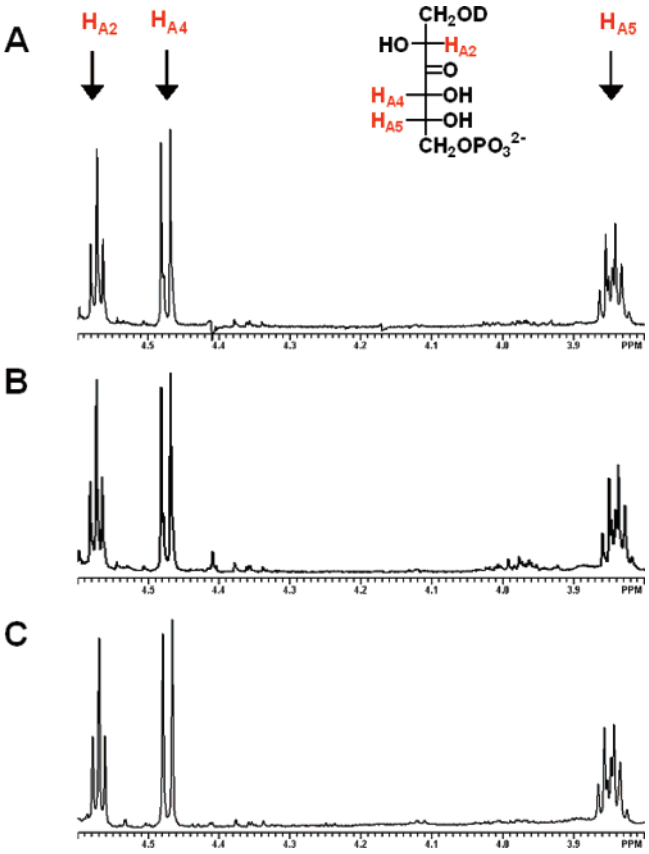

FIGURE 3: Partial ^{1}H NMR spectrum of D-*arabino*-hex-3-ulose 6-phosphate obtained from aldol condensation between D-ribulose 5-phosphate and formaldehyde in D_2O using (A) wild-type HPS, (B) wild-type KGPDC, and (C) the E112D/R139V/T169 mutant of KGPDC.

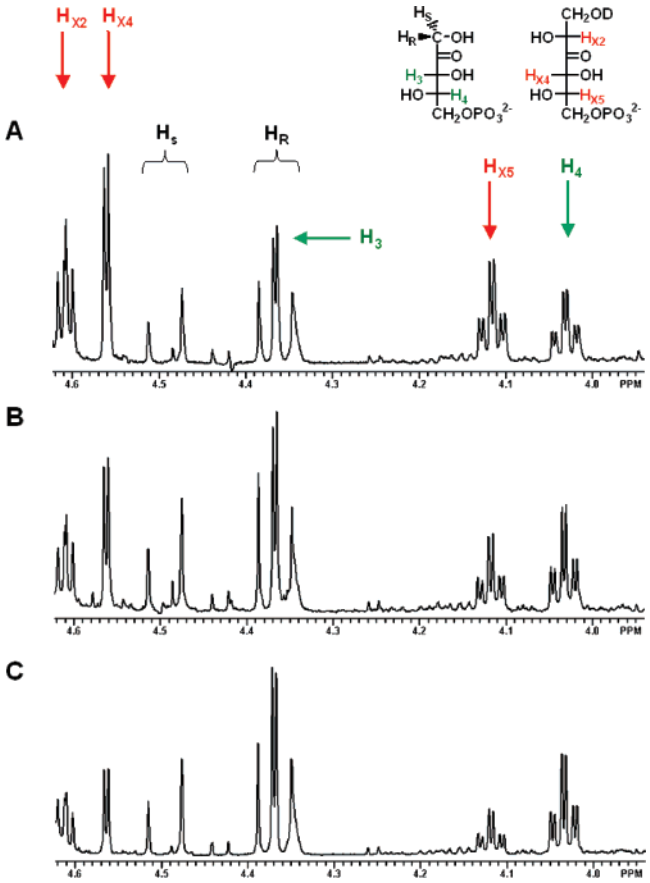

FIGURE 4: Partial ^{1}H NMR spectrum of the product obtained from aldol condensation between L-xylulose 5-phosphate and formaldehyde in D_2O using (A) wild-type HPS, (B) wild-type KGPDC, and (C) the E112D/R139V/T169A mutant of KGPDC.

A comparison of the sequences of orthologous HPS's and KGPDC's reveals strict conservation of several key residues in the active site of KGPDC from *E. coli*, (Figure 2): metal-ion binding ligands, Asp 11 (an indirect ligand via a water molecule), Glu 33, and Asp 62 at the C-terminal ends of the first, second, and third β-strands, respectively; the *cis*-enediolate stabilizing ligands, Lys 64 and Asp 67, at the end of the third β-strand; and the catalytic His 136 at the end of the sixth β-strand (*7*−*9*).

However, the active sites are predicted to differ in the identity of the acidic residue at the end of the fifth β-strand, Glu 112 in KGPDC and its orthologues and an Asp in the HPS's. In KGPDC, Glu 112 and His 136 form a hydrogen-bonded dyad, in which the cationic charge on His 136 is thought to position and promote the acidity of a hydrogen-bonded water molecule that competes for protonation of the 1,2-enediolate intermediate with a second water molecule on the opposite face of the intermediate (*8*, *9*). However, in the HPS-catalyzed reaction, the homologue of His 136 may directly catalyze abstraction of a proton from the 1-hydroxymethylene group of D-ribulose 5-phosphate to generate the nucleophilic 1,2-enediolate intermediate. Consistent with this hypothesis, HPS is more efficient than KGPDC in catalyzing exchange of a proton of the 1-hydroxymethylene groups of both D-ribulose 5-phosphate and L-xylulose 5-phosphate with solvent.

KGPDC contains a strictly conserved Arg 139 at the end of the sixth β-strand. Our previous studies have also implicated the cationic charge on this residue in positioning and promoting the acidity of a proximal water molecule that competes for protonation of the 1,2-enediolate intermediate (*8*, *9*). This functional group is not conserved in the HPS's, where it usually is a hydrophobic residue.

Two residues directly contact L-xylulose 5-phosphate in the active site of KGPDC (*9*). Thr 169 at the end of the seventh β-strand is hydrogen bonded to the hydroxyl group of C4 of the product and could confer specificity to L-xylulose 5-phosphate relative to D-ribulose 5-phosphate (L-xylulose 5-phosphate and D-ribulose 5-phosphate are epimers at C4); in the HPS's this residue is an Ala. Additionally, Arg 192 at the end of the eighth β-strand is hydrogen bonded to the phosphate group of L-xylulose 5-phosphate and could also be involved in conferring substrate specificity; this residue is also an Ala in the HPS's.

Kinetic Parameters of Active Site Mutants. We constructed single and multiple mutants of KGPDC involving the residues described in the previous section; the identities of the various mutants and the values of their kinetic constants for the aldol-condensation reaction between D-ribulose 5-phosphate and formaldehyde are shown in Table 2.

The phenotypes of these mutants were consistent with our predictions:

(1) The H136A substitution eliminated all HPS activity, establishing a crucial catalytic role for the conserved His residue at the end of the sixth β-strand. In KGPDC, His 136 (or a hydrogen-bonded water) functions as the general base that catalyzes stereospecific abstraction of the 1-pro*S* proton

Table 2: Kinetic Parameters of Aldol Condensation between D-Ribulose 5-Phosphate and Formaldehyde

	k_{cat} (s^{-1})	rel k_{cat}	K_M (M)	k_{cat}/K_M (M^{-1} s^{-1})	rel k_{cat}/K_M
wild-type HPS	7.4	n.a.	4.6×10^{-4}	1.6×10^{4}	n.a.
wild-type KGPDC	2.1×10^{-3}	1	2.5×10^{-2}	8.2×10^{-2}	1
H136A	~0			~0	
E112D	4.0×10^{-3}	2	1.4×10^{-2}	2.9×10^{-1}	4
R139V	1.0×10^{-2}	5	2.0×10^{-2}	5.1×10^{-1}	6
T169A	1.0×10^{-2}	5	3.9×10^{-2}	2.5×10^{-1}	3
R192A	$\leq 2.1 \times 10^{-5}$	≤ 0.01			
E112D/R139V	5.6×10^{-2}	27	1.5×10^{-2}	3.7	45
E112D/T169A	4.0×10^{-2}	19	7.3×10^{-3}	5.5	67
R139V/T169A	7.2×10^{-2}	34	7.2×10^{-3}	10	120
E112D/R139V/T169A	0.11	52	5.2×10^{-3}	21	260
E112D/R139V/T169A/R192A	0.36	170	4.0×10^{-2}	9	110

of the 1-hydroxymethylene group of L-xylulose 5-phosphate, so it is expected that this residue will catalyze the proton abstraction of the 1-hydroxymethylene group of D-ribulose 5-phosphate to initiate the HPS reaction.

(2) Single substitutions of E112D, R139V, and T169A produced modest increases in HPS activity (2−5-fold increases in k_{cat} and 3−6-fold increases in k_{cat}/K_M relative to wild-type KGPDC). Double and triple combinations of these single substitutions produced synergistic increments in activity, with the triple mutant (E112D/R139V/T196A) displaying a 52-fold increase in k_{cat} and a 260-fold increase in k_{cat}/K_M relative to wild-type KGPDC.

The R192A substitution dramatically decreased HPS activity. As a result, we did not construct all of the possible double and triple mutants containing the R192A substitution. However, we did construct the E112D/R139V/T196A/R192A quadruple mutant: the value of k_{cat} was increased 3-fold relative to the E112D/R139V/T196A triple mutant, but the value of k_{cat}/K_m was diminished more than 2-fold. Given the contrasting effects of the R192A substitution on the kinetic constants for the E112D/R139V/T196A/R192A, our further mechanistic analyses (vide infra) of the enhanced HPS reaction focused on the E112D/R139V/T196A triple mutant.

(3) Although we did not assay all of the mutants for KGPDC activity, the value of k_{cat}/K_m was decreased a modest 30-fold in the triple mutant and a larger 500-fold for the quadruple mutant, demonstrating the contrasting importance of these residues in the KGPDC reaction. The structural studies reported in the accompanying manuscript provide possible explanations for the reduced KGPDC activities catalyzed by the mutant proteins (*16*).

Thus, we have demonstrated that a "simplistic" redesign of the KGPDC active site scaffold by incorporating the conserved active site functional groups in HPS's is sufficient to significantly increase the ability of the modified KGPDC's to catalyze the promiscuous HPS reaction. Given that the HPS from *M. aminofaciens* is able to catalyze an efficient KGPDC reaction, the relative lack of importance of the mutated residues in supporting the efficiency of the KGPDC reaction is not surprising.

Production of D-arabino-Hex-3-ulose 6-Phosphate by the E112D/R139V/T169A Triple Mutant. Although the promiscuous HPS activity of the E112D/R139V/T196A mutant was increased substantially relative to wild-type KGPDC, it is still significantly less active than the authentic HPS. However, if the substitutions allowed the formation of a diastereomeric mixture of aldol-condensation products, i.e., D-*ribo*-hex-3-ulose 6-phosphate as well as the "natural" D-*arabino*-hex-3-ulose 6-phosphate, the total aldol-condensation activity could be greater than that detected in our assays and reported in Table 2. Accordingly, we utilized ^{1}H NMR spectrometry to establish the identity of the product(s) of the aldol-condensation reaction between D-ribulose 5-phosphate and formaldehyde catalyzed by the E112D/R139V/T169A mutant. We observed the formation of one product, D-*arabino*-hex-3-ulose 6-phosphate, the same product obtained in the reaction catalyzed by the HPS from *M. aminofaciens* (Figure 3).

Role of the Catalytic Histidine at the End of the Sixth β-Strand. The mechanism of the HPS-catalyzed reaction requires proton abstraction from the 1-hydroxymethylene group of D-ribulose 5-phosphate to generate the enediolate intermediate; subsequent condensation of the intermediate with formaldehyde yields the product. We previously attributed the stereospecific exchange of the 1-pro*S* proton of the 1-hydroxymethylene group of L-xylulose 5-phosphate catalyzed by KGPDC to the conjugate base of His 136 (*8*), and given the conservation of this residue in HPS, we surmised that the catalytic base of HPS must be the conserved His at the end of the sixth β-strand.

We observed stereospecific exchange of the 1-pro*S* proton of the 1-hydroxymethylene group of L-xylulose 5-phosphate by HPS and, as expected, also observed exchange of one proton (presumably, the 1-pro*S* proton) of the 1-hydroxymethylene group of D-ribulose 5-phosphate by HPS (Figure 5). Wild-type KGPDC, and the various mutants of KGPDC, with the exception of H136A, were also able to catalyze stereospecific exchange of the 1-pro*S* proton of the 1-hydroxymethylene group of D-ribulose 5-phosphate (Figure 5). These observations are consistent with His 136 directly acting as the catalytic base in the HPS reaction, in contrast to the indirect role of His 136 in protonating the enediolate intermediate in the KGPDC reaction.

Stereochemical Course of the Decarboxylation Reaction Catalyzed by HPS and the E112D/R139V/T169A Mutant. KGPDC catalyzes a non-stereospecific decarboxylation of 3-keto-L-gulonate 6-phosphate, exhibiting a 2:1 ratio of stereoselectivity for proton incorporation on the *si*-face over the *re*-face of C1 of the enediolate intermediate (*8*). We wondered if the promiscuous KGPDC activity exhibited by HPS would follow a stereochemical course similar to that of wild-type KGPDC, or if divergence of function would have resulted in a distinct stereochemical profile.

When 3-keto-L-gulonate 6-phosphate was decarboxylated by wild-type HPS in D_2O buffer, only [1S-^{2}H]-L-xylulose 5-phosphate was produced (Figure 6). The stereochemical course of decarboxylation to yield [1S-^{2}H]-L-xylulose 5-phosphate is inversion of configuration, and is consistent with the observed stereospecific exchange of the 1-pro*S* hydrogen of L-xylulose 5-phosphate with solvent hydrogen. The stereospecificity of this decarboxylation reaction is in striking contrast to the nearly stereorandom decarboxylation of 3-keto-L-gulonate 6-phosphate catalyzed by KGPDC (*8*). The stereospecificity of this reaction may be evidence that the conserved His residue at the end of the fifth β-strand in HPS mediates direct proton transfers to the Mg^{2+}-stabilized *cis*-enediolate intermediate rather than using an intervening water

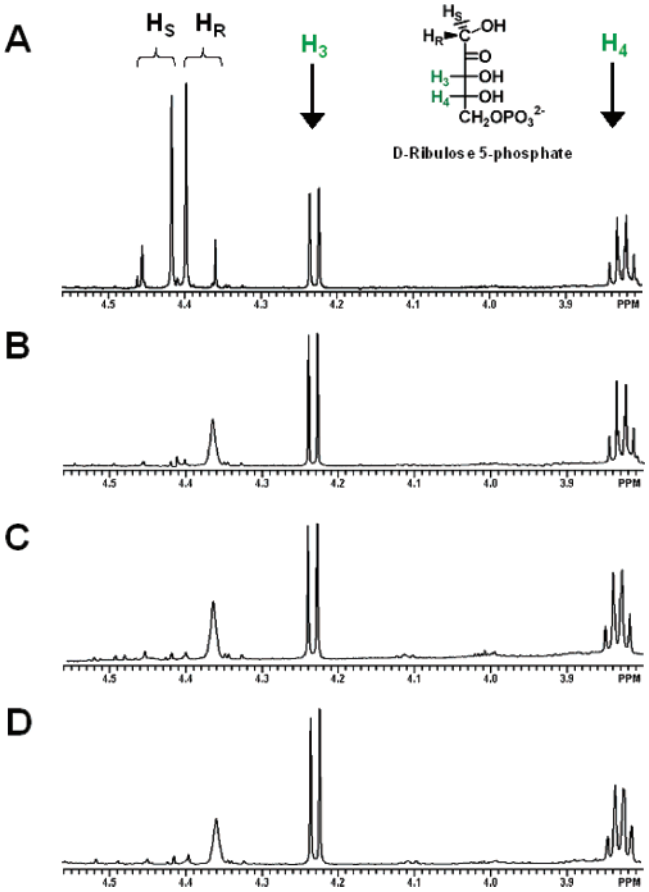

FIGURE 5: (A) Partial ^{1}H NMR spectrum of D-ribulose 5-phosphate showing the assignments of the 1-hydroxymethylene protons. Partial ^{1}H NMR spectrum of D-ribulose 5-phosphate after incubation with (B) wild-type HPS, (C) wild-type KGPDC, and (D) the E112D/R139V/T169A mutant of KGPDC.

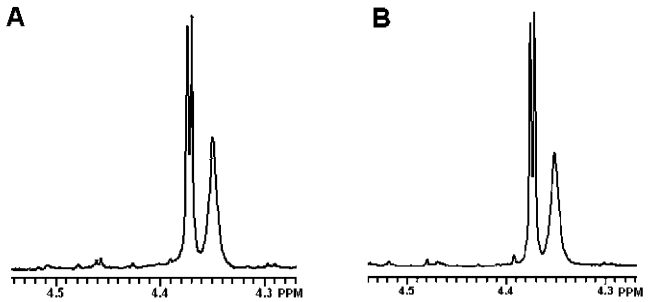

FIGURE 6: Partial ^{1}H NMR spectrum of L-xylulose 5-phosphate obtained from the decarboxylation of 3-keto-L-gulonate 6-phosphate in D_2O using (A) wild-type HPS and (B) the E112D/R139V/T169A mutant of KGPDC.

molecule to deliver a proton to the intermediate, as in the reaction catalyzed by KGPDC. We note that the absence of a homologue of the Arg 139 is expected to decrease the acidity of any water molecule located on the *re*-face of C1 of the intermediate, thereby further favoring the observed stereospecific protonation of the enediolate intermediate derived from decarboxylation.

Interestingly, we observed that the decarboxylation of 3-keto-L-gulonate 6-phosphate catalyzed by the E112D/R139V/T169A mutant is also stereospecific (Figure 6). Again, the absence of Arg 139 is expected to decrease the acidity of any water molecule located on the *re*-face of C1 of the intermediate.

We probed the geometry of the enediolate intermediate by using the facial access of the enediolate intermediate to formaldehyde. The same diastereomer of L-hex-3-ulose 6-phosphate was produced by HPS, wild-type KGPDC, and the E112D/R139V/T169A mutant when 3-keto-L-gulonate 6-phosphate was decarboxylated in the presence of formaldehyde (data not shown). This is persuasive evidence that a *cis*-enediolate intermediate is formed by KGPDC, HPS, and the E112D/R139V/T169A mutant, and that stereochemical divergence occurs at the protonation step.

Catalytic Constraints Imposed by the KGPDC Scaffold? As described in the accompanying manuscript (*16*), structures of wild-type KGPDC and its E112D/R139V/T169A mutant complexed with D-ribulose 5-phosphate reveal an altered binding conformation for the substrate, particularly at the hydroxyl of C-4. This difference in substrate binding can be attributed to the absence of the hydroxyl side chain of Thr 169 and is consistent with the observed 5-fold decrease in K_M for D-ribulose 5-phosphate for the triple mutant. Although the E112D substitution was constructed in an effort to convert the His-Glu dyad conserved in KGPDC's to the His-Asp dyad conserved in HPS's, superposition of the structures of wild-type KGPDC and its E112D/R139V/T169A mutant revealed only a modest change in the position of the imidazole side chain of His 136.

Our sequence-based redesign of the active site of KGPDC produced a remarkable 260-fold increase in catalytic efficiency of HPS activity, but the level of the resulting HPS activity is still $\sim 10^3$-fold less than that observed for the wild-type HPS from *M. aminofaciens*. Despite the modest increase in binding affinity of D-ribulose 5-phosphate, the similar positions of the His-Asp dyad and the His-Glu dyad relative to C1 of D-ribulose 5-phosphate (where proton abstraction occurs to initiate the HPS reaction) likely provide the explanation for the lower activity of the KGPDC mutant relative to the wild-type HPS.

CONCLUSIONS

Both wild-type KGPDC and wild-type HPS are naturally promiscuous for both the decarboxylase and aldol-condensation reactions. The modest HPS activity catalyzed by KGPDC can be enhanced significantly by changing the identities of as few as four active site residues to those conserved in HPS's. The structural data reported in the accompanying manuscript reveal only subtle changes in active site structure as a result of the substitutions (*16*), thereby highlighting the ease by which new functions can evolve in the active sites of members of the OMPDC suprafamily. Our findings complement those previously reported by our laboratories (*17*) and others (*18*, *19*) that only a small number of mutations are required to either introduce or enhance functional promiscuity in enzymes that possess the $(\beta/\alpha)_8$-barrel fold.

REFERENCES

1. Nagano, N., Orengo, C. A., and Thornton, J. M. (2002) One fold with many functions: the evolutionary relationships between TIM barrel families based on their sequences, structures and functions, *J. Mol. Biol. 321*, 741−65.
2. Hughes, A. L. (1994) The evolution of functionally novel proteins after gene duplication, *Proc. R. Soc. London, Ser. B 256*, 119−24.
3. O'Brien, P. J., and Herschlag, D. (1999) Catalytic promiscuity and the evolution of new enzymatic activities, *Chem. Biol. 6*, R91−R105.

4. Wise, E., Yew, W. S., Babbitt, P. C., Gerlt, J. A., and Rayment, I. (2002) Homologous (beta/alpha)8-barrel enzymes that catalyze unrelated reactions: orotidine 5′-monophosphate decarboxylase and 3-keto-L-gulonate 6-phosphate decarboxylase, *Biochemistry 41*, 3861−9.
5. Yew, W. S., and Gerlt, J. A. (2002) Utilization of L-ascorbate by Escherichia coli K-12: assignments of functions to products of the yjf-sga and yia-sgb operons, *J. Bacteriol. 184*, 302−6.
6. Kato, N., Ohashi, H., Hori, T., Tani, Y., and Ogata, K. (1977) Properties of 3-hexulose phosphate synthase and phospho-3-hexuloisomerase of a methanol-utilizing bacterium, 77a, *Agric. Biol. Chem. 188*, 397−401.
7. Wise, E. L., Yew, W. S., Gerlt, J. A., and Rayment, I. (2003) Structural evidence for a 1,2-enediolate intermediate in the reaction catalyzed by 3-keto-L-gulonate 6-phosphate decarboxylase, a member of the orotidine 5′-monophosphate decarboxylase suprafamily, *Biochemistry 42*, 12133−42.
8. Yew, W. S., Wise, E., Rayment, I., and Gerlt, J. A. (2004) Evolution of enzymatic activities in the orotidine 5′-monophosphate decarboxylase suprafamily: mechanistic evidence for a proton relay system in the active site of 3-keto-L-gulonate 6-phosphate decarboxylase, *Biochemistry 43*, 6427−37.
9. Wise, E., Yew, W. S., Gerlt, J. A., and Rayment, I. (2004) Evolution of Enzymatic Activities in the Orotidine 5′-Monophosphate Decarboxylase Suprafamily: Crystallographic Evidence for a Proton Relay System in the Active Site of 3-Keto-L-Gulonate 6-Phosphate Decarboxylase, *Biochemistry 43*, 6438−46.
10. Yanase, H., Ikeyama, K., Mitsui, R., Ra, S., Kita, K., Sakai, Y., and Kato, N. (1996) Cloning and sequence analysis of the gene encoding 3-hexulose-6-phosphate synthase from the methylotrophic bacterium, Methylomonas aminofaciens 77a, and its expression in Escherichia coli, *FEMS Microbiol. Lett. 135*, 201−5.
11. Touster, O. (1962) D- and L-threo-Pentulose (D- and L-xylulose): pyridine-catalyzed epimerization of xylose, *Methods Carbohydr. Chem. 1*, 98−101.
12. Arfman, N., Bystrykh, L., Govorukhina, N. I., and Dijkhuizen, L. (1990) 3-Hexulose-6-phosphate synthase from thermotolerant methylotroph Bacillus C1, *Methods Enzymol. 188*, 391−7.
13. Yasueda, H., Kawahara, Y., and Sugimoto, S. (1999) Bacillus subtilis yckG and yckF encode two key enzymes of the ribulose monophosphate pathway used by methylotrophs, and yckH is required for their expression, *J. Bacteriol. 181*, 7154−60.
14. Winkelman, J., and Ashwell, G. (1961) Enzymic formation of L-xylulose from b-keto-L-gulonic acid, *Biochim Biophys Acta 52*, 170−5.
15. Sahm, H., Schutte, H., and Kula, M. R. (1976) Purification and properties of 3-hexulosephosphate synthase from Methylomonas M 15, *Eur. J. Biochem. 66*, 591−6.
16. Wise, E. L., Yew, W. S., Akana, J., Gerlt, J. A., and Rayment, I. (2005) Evolution of Enzymatic Activities in the Orotidine 5′-Monophosphate Decarboxylase Suprafamily: Structural Bases for Catalytic Promiscuity in Wild-Type and Designed Mutants of 3-Keto-L-gulonate 6-Phosphate Decarboxylase, *Biochemistry 44*, 1816−1823.
17. Schmidt, D. M., Mundorff, E. C., Dojka, M., Bermudez, E., Ness, J. E., Govindarajan, S., Babbitt, P. C., Minshull, J., and Gerlt, J. A. (2003) Evolutionary potential of (beta/alpha)8-barrels: functional promiscuity produced by single substitutions in the enolase superfamily, *Biochemistry 42*, 8387−93.
18. Jurgens, C., Strom, A., Wegener, D., Hettwer, S., Wilmanns, M., and Sterner, R. (2000) Directed evolution of a (beta/alpha)8-barrel enzyme to catalyze related reactions in two different metabolic pathways, *Proc. Natl. Acad. Sci. U.S.A. 97*, 9925−30.
19. Joerger, A. C., Mayer, S., and Fersht, A. R. (2003) Mimicking natural evolution in vitro: an N-acetylneuraminate lyase mutant with an increased dihydrodipicolinate synthase activity, *Proc. Natl. Acad. Sci. U.S.A. 100*, 5694−9.

BI047815V